J Mater Sci (2010) 45:3433–3437
DOI 10.1007/s10853-010-4369-8

Characterization of different work hardening behavior in AISI 321 stainless steel and Hadfield steel

Wanhu Zhang · Junliang Wu · Yuhua Wen · Jianjian Ye · Ning Li

Received: 9 December 2009 / Accepted: 1 March 2010 / Published online: 11 March 2010

Abstract In order to distinguish the difference between AISI 321 stainless steel and Hadfield steel in work hardening behavior, both the Hollomon analysis and the differential Crussard–Jaoul analysis were used to determine the strain hardening exponent as a function of the strain. The results showed that the differential Crussard–Jaoul analysis characterized the discrepancy between AISI 321 steel and Hadfield steel in work hardening behavior more accurately than the Hollomon analysis. The work hardening of AISI 321 stainless steel resulted mainly from interactions of dislocations. When the true strain was rather low, the work hardening of Hadfield steel also resulted mainly from interactions of dislocations. At high strains, twinning would occur in Hadfield steel. It was the occurrence of twins that led to unusual work hardening at larger strains in Hadfield steel.

Introduction

Austenitic steels with low stacking fault energy (SFE), typical example of which include the AISI 321 stainless steel and Hadfield steel, are able to work hardening rapidly at room temperature. It is well known that the work hardening behaviors of austenitic steels are related mainly to stacking fault energy and the lower SFE, the greater work hardening [1]. The SFE of Hadfield steel is 50 mJ/m^2 [1] and that of AISI 321 stainless steel is less than 20 mJ/m^2 [2]. Therefore, it seems to be convincible that AISI 321 stainless steel should have better work hardening ability than Hadfield steel. However, under heavy impact stress Hadfield steel exhibits unique work hardening and higher gouging wear resistance, which is not found in AISI 321 stainless steel. To date, little work has been done to explain this discrepancy.

Strain hardening exponent n is a key parameter for characterizing the work hardening behaviors of metals and alloys. The greater the value of n is, the greater the work hardening. The value of n is determined the most commonly by the Hollomon analysis based on Hollomon's equation, $\sigma = K\varepsilon^n$, where σ is the true stress, ε the total true strain and K a constant [3]. In other words, the value of n is determined from the slope of ln σ versus ln ε curve. For the most of metallic alloys, the value of n determined by the Hollomon analysis is considered a constant. However, although the difference in work hardening behavior between AISI 321 and Hadfield steel exists, the n value of AISI 321 steel determined by Hollomon analysis is around 0.48, being almost equal to that of Hadfield steel [2]. Obviously, the Hollomon analysis cannot distinguish the difference between AISI 321 stainless steel and Hadfield steel in work hardening behavior. Moreover, studies already showed that a single n value cannot represent an entire ln σ–ln ε relation [4]. Therefore, it is necessary to attain the instantaneous slope of the ln σ–ln ε curve to reflect the change of n value with the strain.

Differential Crussard–Jaoul (C–J) analysis was also used to determine the strain hardening exponent n based on Ludwik relation, $\sigma = \sigma_0 + K\varepsilon^n$, where σ_0 and K are a constant [3]. In addition, some researches showed that the change of n value determined by the differential Crussard–Jaoul analysis could relate the work hardening behaviors of metals to the change in microstructures and plastic deformation mechanisms better than that determined by the Hollomon analysis [5–7]. Therefore, it is possible to

W. Zhang · J. Wu · Y. Wen (✉) · J. Ye · N. Li
College of Manufacturing Science and Engineering, Sichuan University, Chengdu 610065, People's Republic of China
e-mail: wenyh-mse@126.com

explain the above discrepancy between AISI 321 stainless steel and Hadfield steel in work hardening behavior using the differential Crussard–Jaoul analysis.

In this paper, it was our aim to distinguish the difference between AISI 321 stainless steel and Hadfield steel in work hardening behavior using the differential Crussard–Jaoul analysis, especially at large deformation.

Methods of analysis

The Hollomon analysis

The Hollomon analysis assumes that the true stress σ versus total true strain ε curve is described by the power relationship [3]:

$$\sigma = K\varepsilon^{n^{\mathrm{H}}} \tag{1}$$

For the concise distinction between the strain hardening exponent determined by the Hollomon analysis and the differential Crussard–Jaoul analysis respectively, a superscript was used. The logarithmic form of Eq. 1 is:

$$\ln\,\sigma = \ln\,K + n^{\mathrm{H}}\ln\,\varepsilon \tag{2}$$

The value of n^{H} as a function of ε is obtained from the instantaneous slope of the curve. That is to say:

$$n^{\mathrm{H}} = \frac{\mathrm{d}\ln\sigma}{\mathrm{d}\ln\varepsilon} = \frac{\frac{1}{\sigma}\mathrm{d}\sigma}{\frac{1}{\varepsilon}\mathrm{d}\varepsilon} = \frac{\varepsilon\mathrm{d}\sigma}{\sigma\mathrm{d}\varepsilon} \tag{3}$$

The differential Crussard–Jaoul (C–J) analysis

The differential Crussard–Jaoul (C–J) analysis is based on Ludwik relation [3]:

$$\sigma = \sigma_0 + K\varepsilon^{n^{\mathrm{C-J}}} \tag{4}$$

The logarithmic form of Eq. 4, after differentiating with respect to ε, formally establishes the analysis method:

$$\ln\frac{\mathrm{d}\sigma}{\mathrm{d}\varepsilon} = \ln(n^{\mathrm{C-J}}K) + (n^{\mathrm{C-J}} - 1)\ln\varepsilon \tag{5}$$

The value of $(n^{\mathrm{C-J}} - 1)$ as a function of ε is obtained from the instantaneous slope of the $\ln\frac{\mathrm{d}\sigma}{\mathrm{d}\varepsilon} - \ln\varepsilon$ curve. That is to say:

$$n^{\mathrm{C-J}} - 1 = \frac{\mathrm{d}\ln\frac{\mathrm{d}\sigma}{\mathrm{d}\varepsilon}}{\mathrm{d}\ln\varepsilon} = \frac{\frac{\mathrm{d}\varepsilon}{\mathrm{d}\sigma}\frac{\mathrm{d}^2\sigma}{\mathrm{d}\varepsilon^2}\mathrm{d}\varepsilon}{\frac{1}{\varepsilon}\mathrm{d}\varepsilon} = \varepsilon\frac{\mathrm{d}\varepsilon}{\mathrm{d}\sigma}\frac{\mathrm{d}^2\sigma}{\mathrm{d}\varepsilon^2} \tag{6}$$

Thus,

$$n^{\mathrm{C-J}} = \varepsilon\frac{\mathrm{d}\varepsilon}{\mathrm{d}\sigma}\frac{\mathrm{d}^2\sigma}{\mathrm{d}^2\varepsilon} + 1 \tag{7}$$

Experimental procedures

Experimental steels were melted and cast in vacuum induction furnace under argon atmosphere. Chemical compositions of steels are listed in Table 1. The ingot were hot forged to bars 15 mm in diameter, and then bars were austenitized at 1373 K for 40 min, followed by a water quenching. Tested specimens were cylindrical and button headed, with a 50 mm gauge length and a 10 mm gauge diameter. The tensile tests were performed at a strain rate of 6.67×10^{-4} s^{-1}.

Table 1 Chemical compositions of two experimental alloys (wt%)

Alloys	C	Mn	Cr	Ni	Ti	Fe
Hadfield steel	1.10	13.30	–	–	–	Bal.
AISI 321 steel	0.07	–	17.80	7.92	0.52	Bal.

Results

Figure 1 shows the true stress σ versus total true strain ε curve of AISI 321 stainless steel and that of Hadfield steel, in which the elastic section and the close rupture section were cut off. Figure 2 shows the $\ln\sigma$–$\ln\varepsilon$ curve determined from Fig. 1. Obviously, none of the curves shows a linear relation. Therefore, a single n value cannot represent an entire curve. To reflect the change of n value with the strain, it is necessary to attain the instantaneous slope of the $\ln\sigma$–$\ln\varepsilon$ curve. Because both the σ–ε curve and its resultant $\ln\sigma$–$\ln\varepsilon$ curve consist of lots of discrete points, we can calculate the difference quotient $\Delta\sigma$ and $\Delta\varepsilon$ instead of the differentiation $d\sigma$ and $d\varepsilon$ respectively. However, this method will introduce errors. To decrease the errors, we first simulated the σ–ε curve and then calculated the differentiation.

Based on the fitted curves of a polynomial with the third degree (red dash line in Fig. 1), the strain hardening exponent $n^{\mathrm{H}}_{\mathrm{exp}}$ of the experimental AISI 321 stainless steel

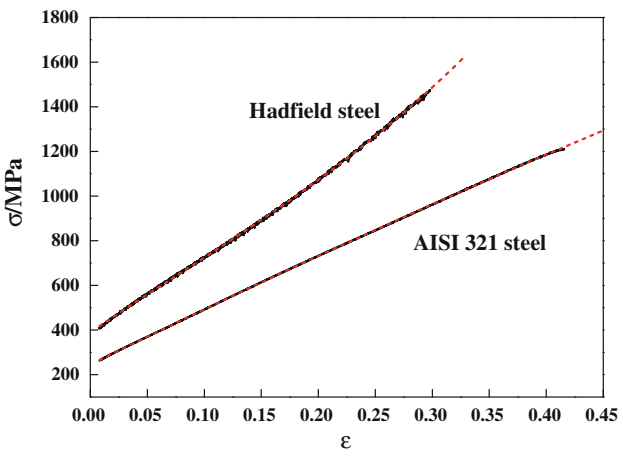

Fig. 1 Experimental and polynomial fitting true stress σ versus total true strain ε curves of AISI 321 stainless steel and Hadfield steel (the elastic section and the close rupture section were cut off; *black solid line* is experimental data, *red dash line* is polynomial fitting data)

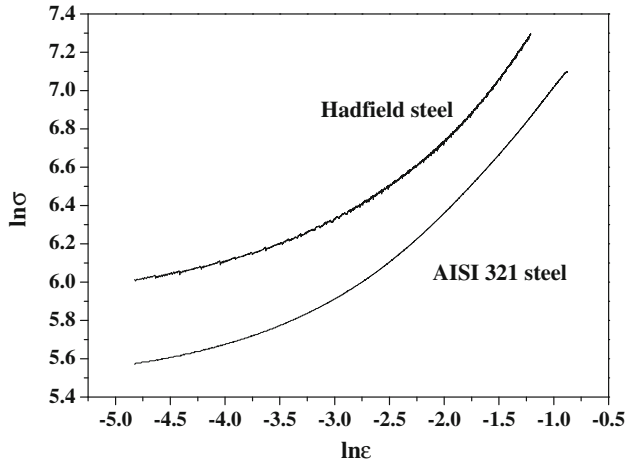

Fig. 2 The ln σ–ln ε curves of AISI 321 stainless steel and Hadfield steel determined from Fig. 1

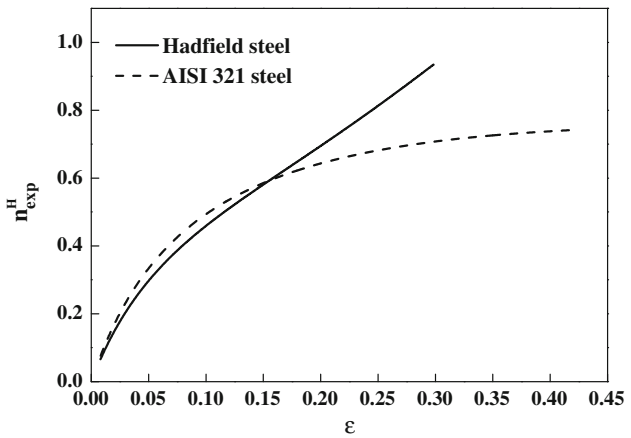

Fig. 3 Strain hardening exponent n^{H}_{exp} determined by Hollomon analysis versus true strain ε curves of AISI 321 stainless steel and Hadfield steel

and Hadfield steel determined by Hollomon analysis are shown in Fig. 3, respectively. Both the n^{H}_{exp} of AISI 321 stainless steel and that of Hadfield steel increased with the strain. Note that when the strain was below about 0.16, the n^{H}_{exp} of AISI 321 stainless steel were almost equal to that of Hadfield steel. When the strain was over 0.16, however, the n^{H}_{exp} of Hadfield steel were greater than that of AISI 321 stainless steel, and the difference between them increased with further increasing the strain.

Figure 4 shows the strain hardening exponent $n^{C–J}_{exp}$ of the experimental AISI 321 stainless steel and Hadfield steel determined by the differential Crussard–Jaoul analysis, respectively. In contrast with the n^{H}_{exp}, the $n^{C–J}_{exp}$ of AISI 321 stainless steel decreased very slowly from 1 with increasing the strain. When the strain was lower than around 0.07, the $n^{C–J}_{exp}$ of Hadfield steel remained constant and was almost equal to that of AISI 321 stainless steel. When the strain was over 0.07, however, it sharply increased with the strain.

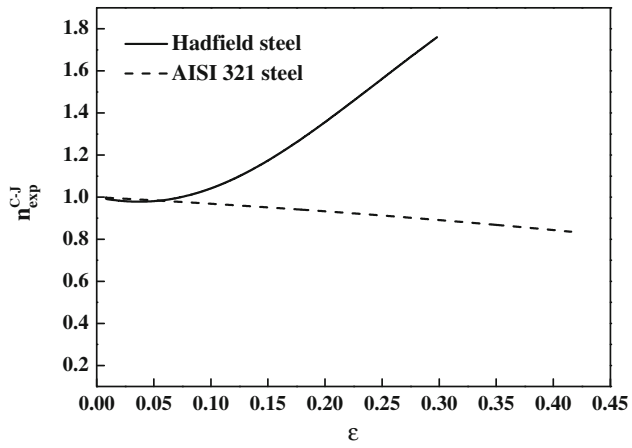

Fig. 4 Strain hardening exponents $n^{C–J}_{exp}$ determined by differential Crussard–Jaoul analysis versus true strain ε curves of AISI 321 stainless steel and Hadfield steel

Discussion

Work hardening is mainly attributed to interactions of dislocations and barriers which impede their motion through the crystal lattice. In addition, it is also confirmed that deformation twinning can result in the high work hardening rate in Hadfield steel [8, 9].

If the deformation is realized only by the dislocation slip, ε is equal to the strain ε_{dis} resulting from dislocation slip. Thompson [10] proposed that the strain increment $d\varepsilon_{dis}$ can be given by the formula as following:

$$d\varepsilon_{dis} = b\lambda d\rho_{dis} \tag{8}$$

where ρ_{dis} is the dislocation density, b the length of the Burgers vector and λ the slip length. Holt and Staker [11] proposed that $\rho_{dis}^{1/2}$ was proportional to the reciprocal of the slip length λ. Thus, Eq. 8 can be rewritten by substituting $\rho_{dis}^{-1/2} = \beta\lambda$, where β is a constant.

$$d\varepsilon_{dis} = b\beta^{-1}\rho_{dis}^{-1/2}d\rho_{dis} \tag{9}$$

ε_{dis} can be obtained through integration of Eq. 9:

$$\varepsilon_{dis} = 2b\beta^{-1}\rho_{dis}^{1/2} \tag{10}$$

Mecking and Kocks [12] proposed the formula relating the stress to the change of dislocation density:

$$\sigma_{dis} = \alpha G b \rho_{dis}^{1/2} \tag{11}$$

where G is the shear modulus, b the length of the Burgers vector and α a constant.

Substituting Eq. 10 into Eq. 11 gives:

$$\sigma_{dis} = \frac{1}{2}\alpha G\beta\varepsilon_{dis} \tag{12}$$

Differentiating Eq. 12 with respect to ε_{dis} yields the strain hardening rates due to interactions of dislocations:

$$\frac{d\sigma_{dis}}{d\varepsilon_{dis}} = \frac{1}{2}\alpha G\beta \tag{13}$$

Thus,

$$\frac{d^2\sigma_{dis}}{d\varepsilon_{dis}^2} = 0 \tag{14}$$

Substituting Eqs. 12 and 13 into Eq. 3 gives:

$$n_{dis}^{H} = \frac{\varepsilon_{dis}d\sigma_{dis}}{\sigma_{dis}d\varepsilon_{dis}} = \frac{2}{\alpha G\beta}\cdot\frac{1}{2}\alpha G\beta = 1$$

Likewise, substituting Eq. 14 into Eq. 7 gives:

$$n_{dis}^{C-J} = \varepsilon_{dis}\frac{d\varepsilon_{dis}}{d\sigma_{dis}}\frac{d^2\sigma_{dis}}{d\varepsilon_{dis}^2} + 1 = 0 + 1 = 1$$

Therefore, the calculated strain hardening exponents resulting only from interactions of dislocations, n_{dis}^{H} and n_{dis}^{C-J}, are both a constant of 1. For experimental AISI 321 stainless steel and Hadfield steel, obviously, the calculated n_{dis}^{H} greatly deviates from their experimental results n_{exp}^{H}. However, the calculated n_{dis}^{C-J} of AISI 321 stainless steel accords well with its experimental result n_{exp}^{C-J}. For Hadfield steel, the calculated n_{dis}^{C-J} also accords well with the n_{exp}^{C-J} when the strain is lower than around 0.07.

If the deformation is realized only by the twining, ε is equal to the strain ε_{twin} resulting from the twining. The strain ε_{twin} can be calculated by the following formula [13]:

$$\varepsilon_{twin} = \ln(1 + \Phi f) \tag{15}$$

where f is the volume fraction of twins and Φ is the equivalent strain provided by twinning and can be evaluated by the formula: $\Phi = S/M$, where S is the twinning shear and M a Taylor factor [13]. Substituting $S = 0.707$ and $M = 3.06$ [14], gives $\Phi = 0.231$.

Differentiating both sides of Eq. 15 with respect to f and substituting $\Phi = 0.231$ gives:

$$d\varepsilon_{twin} = \frac{0.231}{1 + 0.231f}df \tag{16}$$

Remy [15] proposed an expression relating the flow stress σ_{twin} to twinning:

$$\sigma_{twin} = K_T(2t)^{-1}\left(\frac{f}{1-f}\right) \tag{17}$$

where K_T is a constant and t is the average thickness of twins. Thus, the stress increment $d\sigma_{twin}$ is obtained by the differentiation of Eq. 17 with respect to f:

$$d\sigma_{twin} = K_T(2t)^{-1}\frac{1}{(1-f)^2}df \tag{18}$$

Combining Eq. 16 into 18 gives:

$$\frac{d\sigma_{twin}}{d\varepsilon_{twin}} = K_T(2t)^{-1}\frac{1 + 0.231f}{0.231(1-f)^2} \tag{19}$$

Thus,

$$\frac{d^2\sigma_{twin}}{d\varepsilon_{twin}^2} = K_T(2t)^{-1}\frac{(9.658 + f)(1 + 0.231f)}{0.231(1-f)^3} \tag{20}$$

Substituting Eqs. 15, 17 and 19 into Eq. 3 gives n_{twin}^{H}:

$$n_{twin}^{H} = \frac{(1 + 0.231f)\ln(1 + 0.231f)}{0.231f(1-f)} \tag{21}$$

Likewise, substituting Eqs. 15, 19 and 20 into Eq. 7 gives n_{twin}^{C-J}:

$$n_{twin}^{C-J} = \frac{(9.658 + f)\ln(1 + 0.231f)}{(1-f)} + 1 \tag{22}$$

Adler [8] quantified the twined volume fraction f in a Hadfield steel as a function of the total true strain ε, which are summarized in the Table 2. According to f, both the value of n_{twin}^{C-J} and that of n_{twin}^{H} of Hadfield steel were calculated, which is also listed in Table 2.

Figure 5 shows the comparisons between the experimental n_{exp}^{C-J}, calculated n_{dis}^{C-J} and n_{twin}^{C-J} resulting only from dislocation slip and the twinning, respectively. When the strain is lower than 0.05, both the n_{exp}^{C-J} of Hadfield steel and that of AISI 321 stainless steel is almost equal to 1, which coincides with the calculated n_{dis}^{C-J}; when the strain is over 0.05, the n_{exp}^{C-J} of Hadfield steel rapidly increases with the strain, which is coincident with the tendency of the n_{twin}^{C-J}. Note that the n_{twin}^{C-J} of Hadfield steel is greater than the n_{exp}^{C-J} at the same strain. For AISI 321 stainless steel, twinning hardly occurs at room temperature [16], thus its work hardening is mainly attributed to interactions of dislocations with each other.

Remy [15] proposed a twin nucleation model for predicting the critical resolved shear stress:

$$\frac{1}{\sqrt{3}}\left[\frac{1}{3} + K\frac{\tau_T}{G}\right].\frac{\tau_T}{G} = \frac{\gamma}{Gb} \tag{23}$$

Table 2 The comparison between the experimental strain hardening exponent n_{exp}^{H} and n_{exp}^{C-J} and the calculated n_{twin}^{H} and n_{twin}^{C-J} in Hadfield steel

ε_P	f[a]	n_{exp}^{H}	n_{twin}^{H}	n_{exp}^{C-J}	n_{twin}^{C-J}
0.04	0	0.25	1.0	0.98	1.0
0.06	0.05	0.34	1.06	0.98	1.12
0.18	0.18	0.65	1.24	1.28	1.49
0.30	0.25	0.93	1.37	1.76	1.74

[a] The twined volume fraction f was derived from Adler [8]

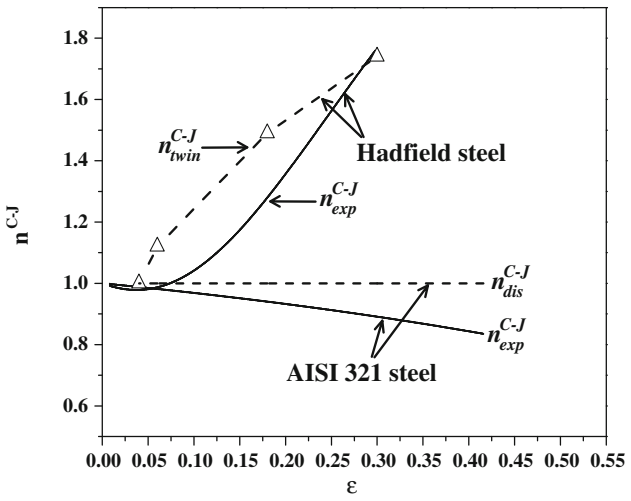

Fig. 5 Comparison between the experimental strain hardening exponents $n_{exp}^{C–J}$, calculated $n_{dis}^{C–J}$ due to dislocations interaction in AISI stainless steel and $n_{twin}^{C–J}$ due to twinning in Hadfield steel

where τ_T is the critical resolved shear stress, γ stacking fault energy, K a constant, G the shear modulus and b the Burgers vector. Substituting $\gamma = 50$ mJ/m^2 [2], $G = 70$ GPa [17] and $K = 700$ [15] into Eq. 23 gives:

$\tau_T = 168.5$ MPa

According to Taylor's theory [14], i.e. $\sigma_C = 3.06\tau_T$, the critical stress σ_C of 515.6 MPa is determined. The corresponding critical strain is around 0.037 determined from Fig. 1. In other words, the twinning cannot take place when the strain is below 0.037 in the present Hadfield steel. Accordingly, the work hardening of Hadfield steel results only from interactions of dislocations with each other when the strain is below 0.037. This result is well agreement with our result that the $n_{exp}^{C–J}$ of Hadfield steel is almost equal to the $n_{dis}^{C–J}$ when the strain is lower than 0.05 (Fig. 5). Twinning will occur when the strain is over 0.037. Therefore, the outstanding work hardening property of high manganese steel at high strain results mainly from the occurrence of twinning. On the other hand, the slip and the twinning are regarded as competing mechanisms. If twinning occurs, it will reorient the crystals lattice, favoring the further basal slip. Thus, deformation will be realized by both slip and twinning. In such a case, the slip length is significantly reduced due to the formation of twins [18], thus cross-slip will readily take place with dislocations pile-up, leading to the occurrence of dynamic recovery and work softening [19]. This may be the reason why the $n_{exp}^{C–J}$ of Hadfield steel is lower than the $n_{twin}^{C–J}$.

Conclusions

The differential Crussard–Jaoul analysis more accurately described and characterized the discrepancy between AISI 321 stainless steel and Hadfield steel in work hardening behavior than the Hollomon analysis. The work hardening of AISI 321 stainless steel mainly resulted from interactions of dislocations. At low strains, the work hardening of Hadfield steel also resulted from interactions of dislocations. When the strain is larger, twinning will occur. It was the occurrence of twinning that led to unusual work hardening at larger strains in Hadfield steel.

Acknowledgements The work was supported by the National Natural Science Foundation of China (No. 50971095) and the Program for New Century Excellent Talents in University (No. NCET-06-0793) and the Key Project of Chinese Ministry of Education (107093).

References

1. Danaf EE, Kalidindi SR, Doherty RD (1999) Metall Mater Trans A 30:1223
2. Dastur YN, Leslie WC (1981) Metall Trans A 12:749
3. Sinha AK (2003) Physical metallurgy handbook. McGraw Hill, Boston
4. Bowen AW, Partridge PG (1974) J Phys D Appl Phys 7:969
5. Soussan A, Degallaix S, Magnin T (1991) Mater Sci Eng A 142:169
6. Umemoto M, Liu ZG, Sugimoto S, Tsuchiya K (1999) Metall Mater Trans A 31:1785
7. Mejia I, Maldonado C, Benito JA, Jorba J, Roca A (2006) Mater Sci Forum 509:37
8. Adler PH, Olson GB, Owen WS (1986) Metall Trans A 17:1725
9. Bayraktar E, Khalid FA, Levaillant C (2004) J Mater Process Technol 147:145
10. Thompson AW, Baskes MI, Flanagan WF (1973) Acta Metall 21:1017
11. Staker MR, Holt DL (1972) Acta Metall 20:569
12. Mecking H, Kocks UF (1981) Acta Metall 29:1865
13. Keshavan MK, Sargent G, Conrad H (1975) Metall Trans A 6:1291
14. Remy L (1981) Metall Trans A 12:387
15. Remy L (1978) Acta Metall 26:443
16. Karaman I, Sehitoglu H, Chumlyakov YI, Maier HJ (2002) J Miner Met Mater Soc 7:31
17. Hutchinson B, Ridley N (2006) Scr Mater 55:299
18. Kalidindi SR (1998) Int J Plast 14:1265
19. Jackson PJ (1985) Prog Mater Sci 29:139